Geochimica et Cosmochimica Acta, Vol. 69, No. 5, pp. 1157–1164, 2005

0016-7037/05 $30.00 + .00

doi:10.1016/j.gca.2004.08.017

Internally consistent database for sulfides and sulfosalts in the system Ag_2S-Cu_2S-ZnS-FeS-Sb_2S_3-As_2S_3: Update

RICHARD O. SACK*
OFM Research, 28430 NE 47th Place, Redmond, Washington 98053-8841 USA

(*Received March* 3, 2004; *accepted in revised form August* 23, 2004)

Abstract—The thermodynamic database for Ag_2S-Cu_2S-ZnS-FeS-Sb_2S_3-As_2S_3 sulfides and sulfosalts applicable to temperatures above 119°C has been updated based on the results of recent petrologic, experimental, and theoretical studies. Solution and end-member properties of fahlore [$\sim(Ag,Cu)_{10}(Fe,Zn)_2(Sb,As)_4S_{13}$] have been adjusted to allow for (1) revisions of the description of Fe-Zn partitioning with sphalerite that incorporate sphalerite activity-composition relations derived from the cluster variation method (CVM) model of a previous study, (2) the assumption that the miscibility gaps observed in high-Ag fahlores from the Husky Mine (Yukon, Canada) approximate a temperature of 170°C, and (3) an increase in the Ag-Cu partitioning between fahlore and polybasite $(Ag,Cu)_{16}(Sb,As)_2S_{11}$ required to reproduce compositions of fahlore in the polybasite + Sb-fahlore + ZnS sphalerite assemblage reported in previous experimental studies. The resulting minor parameter adjustments produce a database that demonstrably reproduces the composition data reported for a wide-range of sulfide ore deposits. They result in revised estimates for the Gibbs energies of formation of end-member fahlore components from the simple sulfides that, except for $Cu_{10}Zn_2Sb_4S_{13}$, are less temperature dependent than those previously inferred (at 200 and 400°C: −23.27 and −24.84 kJ/gfw for $Ag_{10}Zn_2Sb_4S_{13}$, −115.18 and −116.57 kJ/gfw for $Cu_{10}Zn_2Sb_4S_{13}$, −85.14 and −75.20 kJ/gfw for $Cu_{10}Fe_2Sb_4S_{13}$, and −3.81 and 9.10 kJ/gfw for $Ag_{10}Fe_2Sb_4S_{13}$). The database is extended to PbS-bearing supersystems containing the galena + fahlore + sphalerite assemblage. Predicted initial Ag-contents of galena calculated from this database agree with those inferred from petrological studies of Ag-Pb-Zn ores from the Coeur d'Alene district, Idaho, USA and Julcani, Peru. *Copyright © 2005 Elsevier Ltd*

1. INTRODUCTION

An internally consistent thermodynamic database for Ag_2S-Cu_2S-ZnS-FeS-Sb_2S_3-As_2S_3 sulfides and sulfosalts (Sack, 2000) provides a powerful tool for analyzing the petrogenesis of polymetallic, hydrothermal ore deposits and for resource evaluation by mine geologists. It is a database of end-member Gibbs energies and solution models for the Ag_2S-Cu_2S-ZnS-Sb_2S_3 sulfides and sulfosalts highlighted in Figure 1a and for the mixing properties of As- and Fe-substituted varieties of these minerals. Since the publication of this database, petrological studies have been conducted to test its reliability (Sack, 2002; Sack and Goodell, 2002; Sack et al., 2002; Sack et al., 2003; Chutas and Sack, 2004; Sack and Brackebusch, 2004; Sack et al., 2005). These studies have confirmed several predictions. Notably, they have confirmed that the most widely distributed, chemically diverse, and refractory of the sulfosalts, Ag- and Sb-rich tetrahedrite-tennantite fahlore [$\sim(Ag,Cu)_{10}(Fe,Zn)_2(Sb,As)_4S_{13}$], unmixes at temperatures below ~190°C, and that the Ag/(Ag+Cu) ratios of binodal pairs of its miscibility gaps are in accordance with earlier predictions (Sack, 1992; Sack et al., 2003). The data of these new petrological studies also confirm the approximate coordinates of the isotherms for the maximum Ag-contents of fahlores in the Ag_2S-Cu_2S-FeS-ZnS-Sb_2S_3 system (Sack et al., 2002; Sack et al., 2003) and demonstrate that fahlore may be used to accurately define gold fineness and temperatures of hydrothermal mineralization as well as retrograde evolution in Au- and FeS_2-bearing supersystems (Sack and Brackebusch, 2004).

The new petrological data do, however, suggest that some fine-tuning of thermodynamic parameters may improve the database. It appears, for example, that the isotherms for maximal Ag-content of $(Ag,Cu)_{10}(Fe,Zn)_2Sb_4S_{13}$ fahlore (Fig. 2) may be more compressed and displaced slightly higher in molar Ag/(Ag+Cu) at intermediate Zn/(Zn+Fe) (Sack, 2002; Sack et al., 2003). Enrichment in Ag/(Ag+Cu) in fahlores coexisting with polybasite-pearceite [$\sim(Ag,Cu)_{16}(Sb,As)_2S_{11}$] and $(Ag,Cu)_2S$ solid solutions is also implied by phase data from the La Colorada Ag-Zn-Pb deposit, Zacatacas, Mexico (Chutas and Sack, 2004) and 300°C experimental constraints of Ebel (1993) and Sack (2000) for the Ag_2S-Cu_2S-ZnS-Sb_2S_3 subsystem (cf., Fig. 3). Sack (2000) dismissed the inconsistency between the database prediction and the data of Ebel (1993) and Sack (2000) on the grounds that the experiments in question were not reversed.

In this paper we fine-tune and update thermodynamic parameters for fahlore to accomplish these adjustments, and to incorporate activity-composition relations derived from the cluster variation method (CVM) model for (Zn,Fe)S sphalerite of Balabin and Sack (2000) into the database. We then utilize constraints on the mixing properities of argentian galenas (Chutas, 2004) to extend the analysis into PbS-bearing supersystems, and construct a calibration for the Ag-content of galenas coexisting with fahlore and other Ag_2S-Cu_2S-ZnS-FeS-Sb_2S_3-As_2S_3 sulfides and sulfosalts. Finally, we compare these new predictions with the results of the new petrological studies to confirm the validity of the updated database, and to illustrate applications of the database to general problems in economic geochemistry.

* Author to whom correspondence should be addressed (sack@ess.washington.edu).

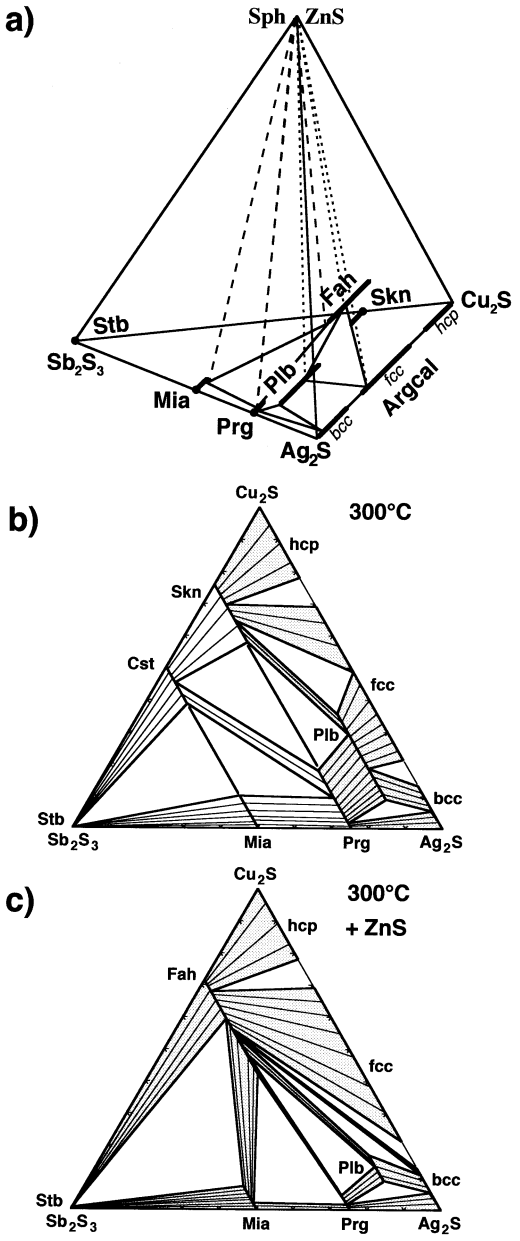

Fig. 1. **a**) Ag_2S-Cu_2S-ZnS-Sb_2S_3 minerals in the database and 300°C phase relations for (**b**) the Ag_2S-Cu_2S-Sb_2S_3 face and (**c**) the sphalerite saturated surface of the tetrahedron. Abbreviations: **hcp**, **fcc**, and **bcc** are hexagonally close packed, face-centered cubic, and body-centered cubic $(Ag,Cu)_2S$ (**Argcal**) solid solutions; **Prg**, pyrargyrite, $\sim(Ag,Cu)_3(Sb,As)S_3$; **Plb**, polybasite, $\sim(Ag,Cu)_{16}(Sb,As)_2S_{11}$; **Mia**, miargyrite, $\sim(Ag,Cu)(Sb,As)S_2$; **Skn**, skinnerite, $\sim(Cu,Ag)_3(Sb,As)S_3$; **Stb**, stibnite, $\sim Sb_2S_3$; **Cst**, chalcostibnite, $\sim(Cu,Ag)(Sb,As)S_2$; **Fah**, fahlore, $\sim(Cu,Ag)_{10}(Zn,Fe)_2(Sb,As)_4S_{13}$; **Sph**, sphalerite, $\sim(Zn,Fe)S$. **a**) Dotted lines illustrate assemblages **Fah + Sph + Prg + Mia** and **Fah + Sph + Plb + Argcal**. **b**) 300°C stability relations for Ag_2S-Cu_2S-Sb_2S_3 sulfides and sulfosalts; stability relations involving **Cst** are schematic and are from Harlov and Sack (1995b). **c**) 300°C stability relations for Ag_2S-Cu_2S-ZnS-Sb_2S_3 sulfides and sulfosalts represented (projected) on the composition plane Ag_2S-Cu_2S-Sb_2S_3. Note reduced **Plb** stability field in (**c**) relative to (**b**) and absence of **Skn** and **Cst** in (**c**).

2. ADJUSTMENT OF THERMODYNAMIC PARAMETERS

In this section the results of fine-tuning of fahlore parameters in the database are reported. The fahlore parameters fine-tuned include (1) solution parameters $\Delta\overline{G}^{*\,\mathrm{Fah}}_{2s}$, $\Delta\overline{G}^{\mathrm{o\,Fah}}_{24}$, and $\Delta\overline{G}^{\mathrm{o\,Fah}}_{34}$; (2) standard-state parameters for Ag-Cu exchange between fahlore and Ag-sulfosalts and sulfides (e.g., $\Delta\overline{H}^{\mathrm{o\,Fah-fcc}}_{\mathrm{Cu(Ag)\text{-}1}}$); and (3) Gibbs energies of formation for the simple sulfides of fahlore end-member components (Table 1). These fahlore parameter values were adjusted without altering parameters in the Ag_2S-Cu_2S-Sb_2S_3-As_2S_3 subsystem, parameters established by Sack (2000) from a voluminous body of studies characterizing phase equilibria (e.g., Skinner, 1966; Harlov and Sack, 1994; Ghosal and Sack, 1995; Harlov and Sack, 1995a; Harlov and Sack, 1995b), calorimetry (e.g., Grønvold and Westrum, 1986; Grønvold and Westrum, 1987; Grønvold et al., 1987; Bryndzia and Kleppa, 1989), and end-member Gibbs energies of formation (e.g., Schenck and von der Forst, 1939; Schenck et al., 1939; Verduch and Wagner, 1957).

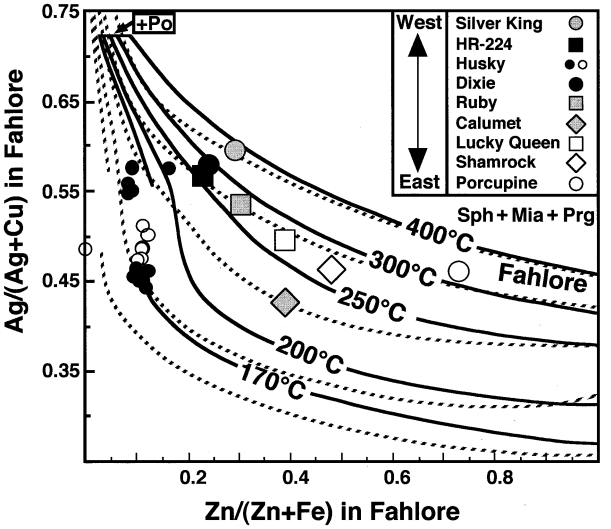

Fig. 2. Molar Ag/(Ag+Cu) and Zn/(Zn+Fe) of high-Ag **Fah** from the Keno Hill Ag-Pb-Zn district, Yukon compared with curves calculated for the maximum solubility of Ag in fahlores in the system Ag_2S-Cu_2S-ZnS-FeS-Sb_2S_3 at 170, 200, 250, 300, and 400°C (**Fah** in equilibrium with **Prg**, **Sph**, and **Mia**). *Dashed curves* are the isotherms calculated by Sack et al. (2002); *solid curves* are the revised isotherms. These isotherms are terminated at low Zn/(Zn+Fe) and high Ag/(Ag+Cu) as a consequence of saturation with respect to pyrrhotite (Po) and this occurs at a roughly constant fahlore Ag/(Ag+Cu) ratio (~0.725) as inferred from the calibration of the sphalerite-hexagonal pyrrhotite two-phase region given by Balabin and Sack (2000, their Figure 4). Larger symbols represent averages for the **Prg**-bearing ores of the western mines (filled symbols) and from the **Prg**-bearing Lucky Queen mine and the adjacent Shamrock and Porcupine mines to the east (open symbols) as calculated by Sack (2002) from data reported by Lynch (1989a). Fluid inclusion, stable isotope, and petrological studies have established that the majority of these primary **Fah**-bearing ores were deposited at temperatures between 250 and 310°C and that most of them retain primary compositions (Lynch, 1989b; Lynch et al., 1990; Sack et al., 2003). Smaller circles represent **Fah** coexisting with stephanite, **Sph**, pyrite and galena (**Gn**) from the Husky Mine that have unmixed into Ag-rich and Ag-poor regions; filled circles represent microprobe analyses obtained by Sack et al. (2003) from relatively Ag-rich and Ag-poor regions of the **Fah** whereas open circles represent intermediate (mixed) compositions.

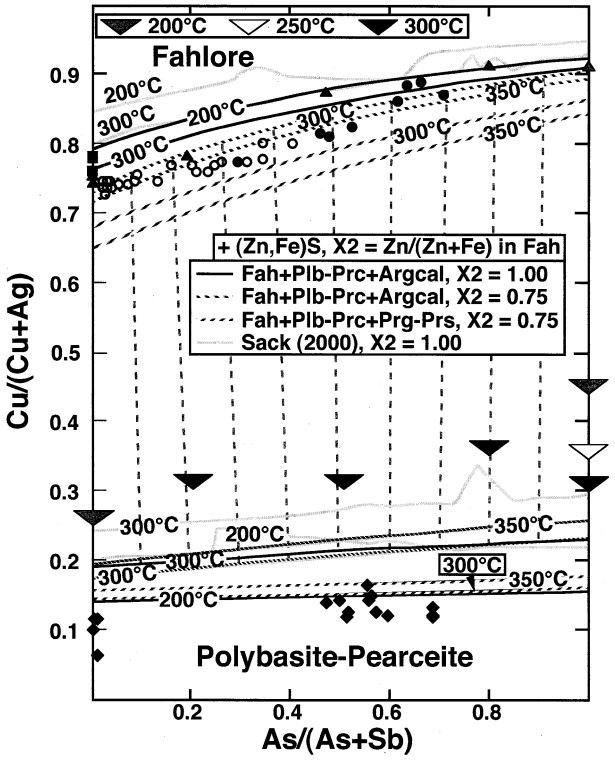

Fig. 3. Calculated molar Cu/(Cu+Ag) and As/(As+Sb) ratios of $(Cu,Ag)_{10}(Fe,Zn)_2(Sb,As)_4S_{13}$ fahlores (**Fah**) and coexisting $(Ag,Cu)_{16}(Sb,As)_2S_{11}$ polybasite-pearceites (**Plb-Prc**) compared with experimental constraints and data from nature. *Darkest and lightest curves* represent compositions of **Fah** and **Plb-Prc** calculated for the assemblage Fah + Plb-Prc + $(Ag,Cu)_2S$ solid solution (**Argcal**) + ZnS sphalerite (**Sph**) at 200 and 300°C using the updated parameters and by Sack (2000), respectively. *Dashed curves* for 300 and 350°C are for this assemblage and for the **Fah** + **Plb-Prc** + pyrargyrite-proustite (**Prg-Prs**) + **Sph** assemblage with molar Zn/(Zn+Fe) in **Fah** of 0.75. *Near vertical dashed lines* are representative calculated tie-lines between coexisting **Fah** and **Plb-Prc** in the assemblage **Fah** + **Plb-Prc** + **Argcal** + **Sph** at 300°C with molar Zn/Zn+Fe) of **Fah** of 0.75. Smaller *arrows pointing upwards* are molar Cu/(Cu+Ag) and As/(As+Sb) ratios of **Fah** coexisting with **Plb-Prc**, **Argcal** and **Sph** in 200 to 300°C experiments in the Ag_2S-Cu_2S-ZnS-Sb_2S_3-As_2S_3 system reported by Sack (2000). Larger *arrows pointing downwards* represent **Plb-Prc** with the lowest Cu/(Cu+Ag) ratios observed to react with **Sph** to form **Fah** and **Argcal** in these experiments; they constitute half brackets on the compositions of **Plb-Prc** in the **Fah + Plb-Prc + Argcal + Sph** assemblage. *Solid squares* are Cu/(Cu+Ag) ratios of **Fah** in this assemblage produced in the 300°C experiments of Ebel (1993) in the Ag_2S-Cu_2S-ZnS-Sb_2S_3 subsystem. *Circles and diamonds* represent Cu/(Cu+Ag) and As/(As+Sb) ratios of **Fah** and **Plb-Prc** in sample NC-11 from the La Colorada Ag-Zn-Pb deposit in Zacatacas, Mexico (Chutas and Sack, 2004). **Fah** occur as inclusions in **Sph**. *Open* and *filled* circles distinguish **Fah** with molar Zn/Zn+Fe) ratios $>$ and $<$0.75. **Argcal** occurs only with **Plb-Prc**; **Prg-Prs** is not observed. **Fah** in NC-11 are assumed to represent a temperature of ~325°C; this is the temperature of deposition deduced for a related **Prg**-bearing sample based on the compositions of high-Ag **Fah** inclusions in quartz and Figure 2, as well as that established from fluid inclusions (Chutas and Sack, 2004). The fact that the **Plb-Prc** from NC-11 have molar Cu/(Cu+Ag) ratios less than those of the calculated **Plb-Prc** curves is believed to reflect the nonquenchable nature of **Plb-Prc** compositions (cf., Harlov and Sack, 1994).

In this study, slightly smaller values of the first two fahlore parameters, ($\Delta\bar{G}^{*\,\mathrm{Fah}}_{2s}$ and $\Delta\bar{G}^{\mathrm{o\,Fah}}_{24}$), were adopted (Table 1). They are permitted by fahlore-sphalerite Fe-Zn partitioning data (Sack and Loucks, 1985; O'Leary and Sack, 1987) and the condition of equilibrium for the Fe-Zn exchange reaction between (Zn,Fe)S sphalerites and $(Cu,Ag)_{10}(Fe,Zn)_2Sb_4S_{13}$ fahlores,

$$\frac{1}{2}Cu_{10}Zn_2Sb_4S_{13} + FeS = ZnS + \frac{1}{2}Cu_{10}Fe_2Sb_4S_{13}, \quad (1)$$

when activity-composition relations of (Zn,Fe)S sphalerites are described by the expressions given by Balabin and Sack (2000), rather than by those given by Sack and Loucks (1985). These downward adjustments of $\Delta\bar{G}^{*\,\mathrm{Fah}}_{2s}$ and $\Delta\bar{G}^{\mathrm{o\,Fah}}_{24}$ are accompanied by a modest upward adjustment of $\Delta\bar{H}^{\mathrm{o\,Fah-fcc}}_{\mathrm{Cu(Ag)\text{-}1}}$ (Table 1), the standard state enthalpy of the Ag-Cu exchange reactions between fahlore (Fah) and $(Ag,Cu)_2S$ solutions with the face-centered cubic structure (fcc),

$$\frac{1}{16}Cu_{10}Zn_2Sb_4S_{11} + \frac{1}{2}Ag_2S = \frac{1}{16}Ag_{10}Zn_2Sb_2S_{11} + \frac{1}{2}Cu_2S. \quad (2)$$

This requires equal upward adjustments of standard state enthalpies for other Ag-Cu exchange reactions between fahlore and the other Ag-sulfosalts and sulfides, such as that between fahlore and polybasite-pearceite (Plb),

$$\frac{1}{16}Ag_{16}Sb_2S_{11} + \frac{1}{10}Cu_{10}Zn_2Sb_4S_{13} = \frac{1}{16}Cu_{16}Sb_2S_{11} + \frac{1}{10}Ag_{10}Zn_2Sb_4S_{13} \quad (3)$$

$\Delta\bar{H}^{\mathrm{o\,Fah-Plb}}_{\mathrm{Cu(Ag)\text{-}1}}$ ($= \Delta\bar{H}^{\mathrm{o\,Fah-fcc}}_{\mathrm{Cu(Ag)\text{-}1}} - \Delta\bar{H}^{\mathrm{o\,Plb-fcc}}_{\mathrm{Cu(Ag)\text{-}1}}$) . Values for the Gibbs energies of formation of $Ag_{10}Zn_2Sb_4S_{13}$ fahlore were revised to take into account the 200°C, 300°C, and 400°C experimental brackets of Ebel and Sack (1994) on the Ag/Cu ratios of fahlores coexisting with pyrargyrite, miargyrite, and ZnS

Table 1. Updated thermodynamic parameters.[a]

Parameter	Value	Revised from
$\Delta\bar{G}^{\mathrm{o\,Fah}}_{24}$	9.00	9.6232
$\Delta\bar{G}^{*\,\mathrm{Fah}}_{2s}$	9.00	10.8784
$\Delta\bar{H}^{\mathrm{o\,Fah\text{-}fcc}}_{\mathrm{Cu(Ag)_{-1}}}$	9.15	8.32
$\Delta\bar{G}^{\mathrm{o\,Fah}}_{34}$	50.34	51.25
$\Delta\bar{H}_f$ $Ag_{10}Zn_2Sb_4S_{13}$	−19.5393	−12.1594
$\Delta\bar{S}_f$ $Ag_{10}Zn_2Sb_4S_{13}$	7.880	17.18
$\Delta\bar{H}_f$ $Cu_{10}Zn_2Sb_4S_{13}$	−119.8472	−104.1717
$\Delta\bar{S}_f$ $Cu_{10}Zn_2Sb_4S_{13}$	−6.928	2.372
$\Delta\bar{H}_f$ $Cu_{10}Fe_2Sb_4S_{13}$	−51.6719	−35.9964
$\Delta\bar{S}_f$ $Cu_{10}Fe_2Sb_4S_{13}$	49.72	59.02
$\Delta\bar{H}_f$ $Ag_{10}Fe_2Sb_4S_{13}$	39.6360	46.3929
$\Delta\bar{S}_f$ $Ag_{10}Fe_2Sb_4S_{13}$	64.53	73.83

[a] Values expressed in kJ/gfw or J/K-gfw; enthalpies and entropies of formation are relative to the stable simple sulfides Ag_2S, Cu_2S, ZnS, FeS, and Sb_2S_3.

sphalerite in the reaction

$$\underset{\text{Ag}-\text{fahlore}}{Ag_{10}Zn_2Sb_4S_{13}} = \underset{\text{pyrargyrite}}{3Ag_3SbS_3} + \underset{\text{miargyrite}}{AgSbS_2} + \underset{\text{sphalerite}}{2ZnS} \quad (4)$$

and new values for the Gibbs energies of formation of the remaining Sb-fahlore end members were obtained following the methods outlined in Sack (2000). Finally, the solution parameter expressing the incompatibility between Ag and As in fahlore for the reaction

$$Cu_{10}Fe_2As_4S_{13} + Ag_{10}Fe_2Sb_4S_{13} = Cu_{10}Fe_2Sb_4S_{13} + Ag_{10}Fe_2As_4S_{13} \quad (5)$$

($\Delta\overline{G}^{o\,Fah}_{34}$), was revised to be consistent with Ebel and Sack's (1989) tightest reversal brackets on the Ag-content of fahlore coexisting with electrum, chalcopyrite, and pyrite (exps. # B2-2, D2-3, D2R-1, E2-1, H2-2, J2-2, S2-1, G4-1, I4-1, K4-1, S4-1, H4-1, L4-1).

Downward adjustments of the fahlore parameters $\Delta\overline{G}^{*\,Fah}_{2s}$ and $\Delta\overline{G}^{o\,Fah}_{24}$ have the desired effects of compressing and raising the isotherms in Figure 2, allowing for a modest increase in $\Delta\overline{H}^{o\,Fah-fcc}_{Cu(Ag)-1}$ (or $\Delta\overline{H}^{o\,Fah-Plb}_{Cu(Ag)-1}$) without shifting the fahlore isotherms in Figure 2 to significantly lower values of Ag/(Ag+Cu) at intermediate-low Zn/(Zn+Fe) ratios. By itself, upward adjustments of $\Delta\overline{H}^{o\,Fah-fcc}_{Cu(Ag)-1}$ are problematic as fluid inclusion, stable isotope, and mineralogical studies (Lynch, 1989a; Lynch, 1989b; Lynch et al., 1990; Sack, 2002; Sack et al., 2003) demonstrate that, if these isotherms need to be adjusted at all, the required adjustments must be in the opposite direction (cf., Fig. 2). Coupled with a decrease in $\Delta\overline{G}^{*\,Fah}_{2s}$, upward adjustment in $\Delta\overline{H}^{o\,Fah-fcc}_{Cu(Ag)-1}$ within the bounds of the original estimate, 8.32 ± 1.17 kJ/gfw (Sack, 2000), has the desired effects of decreasing the Cu/(Cu+Ag) ratios of fahlores in the fahlore + polybasite + sphalerite + $(Ag,Cu)_2S$ assemblage. These adjustments also have the desired effect of bringing the Ag-Cu exchange constraints of Sack (2000) and Ebel (1993) on $\Delta\overline{H}^{o\,Fah-fcc}_{Cu(Ag)-1}$ into closer alignment (cf., Fig. 2 of; Sack, 2000).

Accordingly, $\Delta\overline{G}^{*\,Fah}_{2s}$, $\Delta\overline{G}^{o\,Fah}_{24}$ and $\Delta\overline{H}^{o\,Fah-fcc}_{Cu(Ag)-1}$ were adjusted within the original bounds determined in the earlier works of O'Leary and Sack (1987) and Sack (2000) until the calculated Cu/(Cu+Ag) ratio of fahlore coexisting with polybasite, sphalerite, and $(Ag,Cu)_2S$ in the Ag_2S-Cu_2S-ZnS-Sb_2S_3 system at 300°C (Fig. 3) accorded with the ratios reported by Ebel (1993) and Sack (2000), and, until the 170°C isotherm for reaction (3) on Figure 2 passed through the fahlore miscibility gap pairs reported for a sample from the Husky Mine by Sack et al. (2003). Finally, composition variables of fahlore + polybasite + sphalerite + $(Ag,Cu)_2S$ assemblages based on analysis of the reaction

$$\underset{\text{polybasite}}{2Ag_{16}Sb_2S_{11}} + \underset{\text{sphalerite}}{2ZnS} = \underset{\text{Ag-fahlore}}{Ag_{10}Zn_2Sb_4S_{13}} + \underset{\text{bcc- or fcc-}(Ag,Cu)_2S}{11Ag_2S} \quad (6)$$

were extended to As-bearing polybasite-pearceites and Fe- and As-bearing fahlores (Fig. 3) for comparison with the petrological constraints reported by Chutas and Sack (2004). This procedure was repeated iteratively until an optimal solution was obtained.

Among the consequences of the fine-tuning are a reduced polybasite field (Fig. 1c) and an increase of ~45°C in the calculated temperature at which reaction (6) intersects the bcc- to fcc-$(Ag,Cu)_2S$ transition loop (Fig. 4). In addition to now reproducing the 300°C experimental constraints on the Ag/(Ag+Cu) ratios of fahlore coexisting with polybasite, ZnS sphalerite, and $(Ag,Cu)_2S$, the calculations are also now in significantly better agreement with the Ag/(Ag+Cu) ratios of polybasite and $(Ag,Cu)_2S$ solid solutions reported by Ebel (1993). The new adjustments also provide an excellent accounting for the petrological constraints of Chutas and Sack (2004) (cf., Fig. 3) and result in revised estimates for the Gibbs energies of formation of end-member fahlore components from the simple sulfides (Table 1) that, except for $Cu_{10}Zn_2Sb_4S_{13}$, are less temperature dependent than those inferred by Sack (2000). The revised parameters also result in calculated binode pairs for Zn-bearing Sb-fahlores with slightly higher Ag/(Ag+Cu) ratios as a consequence of the reduced value of $\Delta\overline{G}^{*\,Fah}_{2s}$. This shift, and the miscibility gap pairs reported by Sack et al. (2003), effectively limit how much $\Delta\overline{G}^{*\,Fah}_{2s}$ can be lowered. Attempts to compensate for this effect by adjusting other parameters for Sb-fahlores are not warranted at this point, as these other parameters are either highly constrained or their adjustments have unintended and unacceptable consequences (cf., O'Leary and Sack, 1987; Sack, 1992).

3. DISCUSSION

Our revised estimates for the standard state Gibbs energies of formation of fahlore components, and of the mixing properties of fahlore solutions, constitute an update of the thermodynamic database for end-member and mixing properties of Ag_2S-Cu_2S-ZnS-Sb_2S_3 sulfosalts/sulfides and its extension to a subset of As-bearing argentian sulfosalts, and Fe-rich fahlores and (Zn,Fe)S phases. Comprehensive field testing (Sack, 2002; Sack and Goodell, 2002; Sack et al., 2002; Sack et al., 2003; Chutas and Sack, 2004; Sack and Brackebusch, 2004; Sack et al., 2005) has shown that predictions from this database are generally reliable, and further petrologic and experimental studies should afford the extension of this database downward in temperature and outwards in composition to encompass As- and Fe-bearing systems. There are, of course, many lingering uncertainties within these subsystems that need to be resolved. Several of these were highlighted by Sack (2000), and a few should be mentioned or reiterated here. They include the exact nature of miscibility gaps in Ag-rich fahlores, the characteristics of (Zn,Fe)S "sphalerites" at ore-forming temperatures, the partitioning of Fe and Zn between Ag-rich fahlores and (Zn,Fe)S "sphalerites," and of Ag and Cu between fahlores and polybasite-pearceites.

The first of these issues, the exact nature of miscibility gaps in Ag-rich fahlores, is one that has been discussed in several publications (e.g., O'Leary and Sack, 1987; Sack et al., 1987;

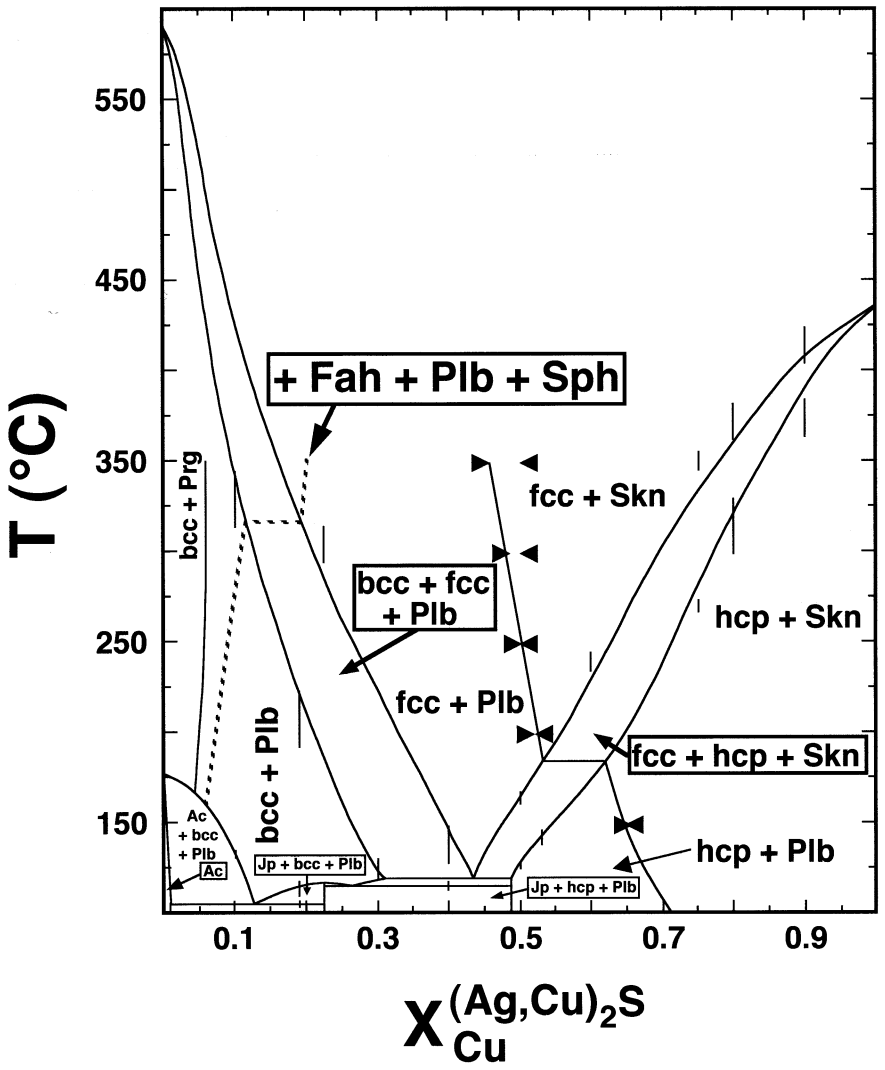

Fig. 4. Temperature-composition diagram for Ag_2S-Cu_2S sulfides coexisting with Ag_2S-Cu_2S-ZnS-Sb_2S_3 sulfosalts, compared with experimental constraints. Solid curves represent calculated two phase loops for **bcc**- + **fcc**- and **fcc**- + **hcp**-$(Ag,Cu)_2S$ assemblages and remaining curves extending above 176°C represent calculated compositions of $(Ag,Cu)_2S$ solutions coexisting with **Prg** + **Plb**, **Plb** + **Skn**, and **Fah** + **Plb** + **Sph**. Phase relations below 119°C are from Skinner (1966). Vertical lines represent temperature-composition constraints inferred by Skinner (1966). Arrows represent brackets on molar Cu/(Cu+Ag) ratios of $(Ag,Cu)_2S$ sulfides coexisting with **Plb** + **Skn** of Harlov and Sack (1995b). Fields are labeled for the $(Ag,Cu)_2S$ sulfide + Ag_2S-Cu_2S-Sb_2S_3 sulfosalt assemblage ignoring phase relations involving stephanite (cf., Keighin and Honea, 1969). **Ac** and **Jp** are abbreviations for acanthite and jalpaite.

Sack, 1992; Sack and Ebel, 1993) before their discovery in Sb-rich fahlores from the Husky Mine (Sack et al., 2003). As noted in these papers, the existence of such gaps cannot be readily reconciled with inferences about the structural role of Ag in fahlores as deduced from spectroscopic studies conducted at, or below, room temperature (cf., Sack, 1992). However, thermochemical analysis successfully predicts the existence of these miscibility gaps and the compositions of binodal pairs. It is time for petrologists to carefully examine sulfide ore deposits for evidence of such gaps in As- and Ag-rich fahlores, where thermochemical analysis indicates they are substantially more extensive than in Sb-rich systems (cf., Sack et al., 2003). Until this latter activity is undertaken, the thermochemical models for As- and Ag-rich fahlores will remain uncertain.

An additional issue of interest is the nature of (Zn,Fe)S phases at ore-forming temperatures. Although it is generally accepted that sphalerites with less than ~15 mol % FeS are stable at temperatures of hydrothermal mineralization, the recent CVM model for the thermodynamic properties of (Zn,Fe)S sphalerites indicates sphalerites with very low Fe-contents may not be stable at temperatures below ~380°C (cf., Fig. 9 of Balabin and Sack, 2000). Balabin and Sack (2000) have also demonstrated that the strong nonadditive interactions in the cation sublattice of (Zn,Fe)S sphalerite, required to account for high-temperature equilibria, also make it unlikely that FeS-rich (Zn,Fe)S phases have the sphalerite structure senso stricto at the temperatures of interest here. Thus, it appears that further petrologic and material properties studies of assemblages bear-

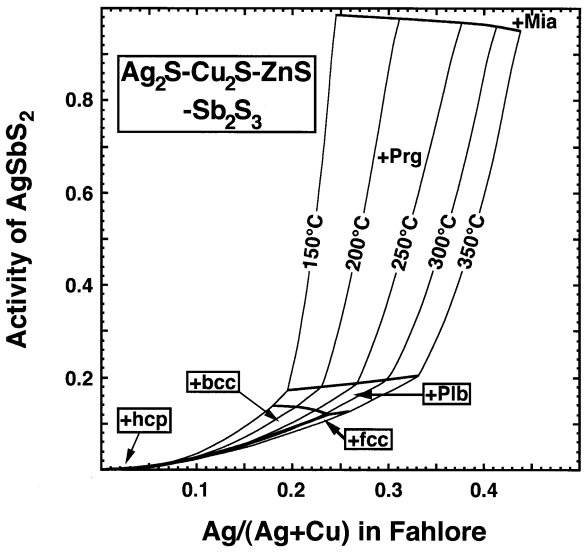

Fig. 5. Activity of $AgSbS_2$ and Ag/(Ag+Cu) values of fahlore in **Fah** + **Sph** + sulfosalt or **Argcal** assemblages over the temperature range 150 to 350°C in the simple system Ag_2S-Cu_2S-ZnS-Sb_2S_3. Activity of $AgSbS_2$ calculated relative to stable end-member $AgSbS_2$. Activities of $AgSbS_2$ in the **Fah** + **Sph** + **Mia** and **Fah** + **Sph** + **Stb** assemblages (Fig. 1c) are not shown.

ing FeS-rich (Zn,Fe)S phases will be required before the database can be accurately extended into Fe-rich systems.

Despite the uncertainties highlighted above, the database is now sufficiently robust that we may consider extending it to more complex systems. An extension to PbS-bearing systems may be used to illustrate the utility of the database in analyzing the petrogenesis of polymetallic, hydrothermal ore deposits and in developing tools for resource evaluation. A case in point is provided by Ag-Pb-Zn ore deposits in which galena coexists with fahlore, sphalerite, and other sulfides and sulfosalts (e.g., Sack and Goodell, 2002; Sack et al., 2002; Sack et al., 2003; Chutas and Sack, 2004; Sack et al., 2005). Addition of galena to the database is straightforward. Galena is typically close to a binary $AgSbS_2$-Pb_2S_2 solid solution, except in Bi-rich deposits where a $AgBiS_2$ substitution becomes important (e.g., Goodell and Petersen, 1974). The chemical potential (or activity) of the $AgSbS_2$ component in galena is defined continuously by the Ag/(Ag+Cu) ratio of fahlore coexisting with sphalerite and pyrargyrite-proustite, polybasite-pearceite, or bcc-, fcc-, or hcp-$(Ag,Cu)_2S$ solid solution (Fig. 5). Given mixing properties for $AgSbS_2$-Pb_2S_2 galena solid solution (Chutas, 2004), the activities of the $AgSbS_2$ component of Figure 5 can be readily translated to mole fractions of $AgSbS_2$ component in galena to produce a corresponding calibration for fahlore Ag/(Ag+Cu) ratio and $AgSbS_2$-mole fraction in galena (Fig. 6). This calibration may then be compared with the results of petrological studies.

The most straightforward comparison is with the galena ores from the Coeur d'Alene district, Idaho (Sack, et al., 2002; Sack, et al., 2005). The $AgSbS_2$ concentration in Coeur d'Alene galena, as with other near-room-temperature $AgSbS_2$-Pb_2S_2 galenas, is presently below the detection limit of the electron microprobe, Ag ~ 0.1 wt. % (e.g., Knowles, 1983; Sack, et al., 2002). Corona textures (Sack, et al., 2002) and mass balance constraints (Hardy, 2002) attest, however, that original $AgSbS_2$ concentrations in Coeur d'Alene galenas were significantly higher, and most of this $AgSbS_2$ was depleted by the reaction

$$\underset{\text{Cu-fahlore}}{\frac{1}{10}Cu_{10}(Zn,Fe)_2Sb_4S_{13}} + \underset{\text{in galena}}{AgSbS_2} + \underset{\text{galena}}{PbS} = \underset{\text{bournonitc}}{CuPbSbS_3} + \underset{\text{Ag-fahlore}}{\frac{1}{10}Ag_{10}(Zn,Fe)_2Sb_4S_{13}} \quad (7)$$

which occurred during cooling following galena mineralization and produced a population of high-Ag fahlores in galena-rich ores. It is, nevertheless, possible to reconstruct the original compositions of galena (and fahlore) from the secondary mineralogy on the assumption of closed system behavior. Sack et al. (2002) determined the increase in the Ag/(Ag+Cu) of fahlore and concurrent depletion of $AgSbS_2$ in galena for two galena-rich ores, one from the West Chance vein of the Sunshine Mine (WC-7) and the other from the Gold Hunter vein of the Lucky Friday Mine (GH-5). Adding to these $AgSbS_2$ depletion estimates an assumed present value of Ag in galena of half the minimum EPMA detection limit (0.05 wt %), estimates for initial compositions (Fig. 6b) are consistent with temperatures of roughly 360 (WC-7) and 290°C (GH-5). These may be compared with a temperature of ~350°C inferred by matching a minimum of ~0.12 wt. % Ag ($X^{Gn}_{AgSbS_2} \sim 0.0053$) for Coeur d'Alene galena ores with a minimum of 0.04 to 0.06 for molar Ag/(Ag+Cu) in Sb-fahlores (e.g., Hackbarth, 1984; Trachte, 1993). The first and last of these estimates are in accord with other estimates for primary mineralization temperatures in the district (e.g., Sack et al., 2005). The lower temperature inferred for GH-5 may well reflect natural variation, more open system behavior during slower cooling of the Golden Hunter than the West Chance ores (Sack et al., 2005), a low estimate for the present Ag concentration in galena, or failure to detect the Ag-Pb-Sb sulfosalt diaphorite (~$Pb_2Ag_3Sb_3S_8$), a sulfosalt that has been discovered in a related Gold Hunter sample (Sack et al., 2002). This lower-temperature estimate does not, therefore, appear to degrade the inference that the calibration is quite adequate.

The calibration also predicts that high-Ag galenas were deposited in some pyrargyrite-bearing mesothermal ores such as those from Julcani, Peru (Sack and Goodell, 2002) and from the Keno Hill Ag-Pb-Zn district, Yukon (Sack et al., 2003). Several relics of such high-Ag galenas (Fig. 6a) are found in ores from the "bonanza-Ag" zone of Julcani (Sack and Goodell, 2002). During retrograde cooling, these primary, Bi-bearing galenas have decomposed into Ag-poor galena, pyrargyrite, aramayoite [~$(Ag,Cu)_5(Sb,Bi)_4(Bi,Sb)S_{10}$, Sb-Bi analog of miargyrite], and, depending on Bi/Sb ratio, either the Ag-Pb-Sb sulfosalt diaphorite [~$Pb_2Ag_3(Sb,Bi)_3S_8$] or its newly discovered Bi-analog bismuthian diaphorite [~$Pb_2Ag_3(Bi,Sb)_3S_8$ (Sack and Goodell, 2002)]. The path of composition change for the most Bi-poor galenas can be roughly approximated as shown schematically in Figure 6a. At Julcani, pyrargyrite-forming reactions that occurred during cooling and galena retrogradation provide a source for the semimetal sulfides that

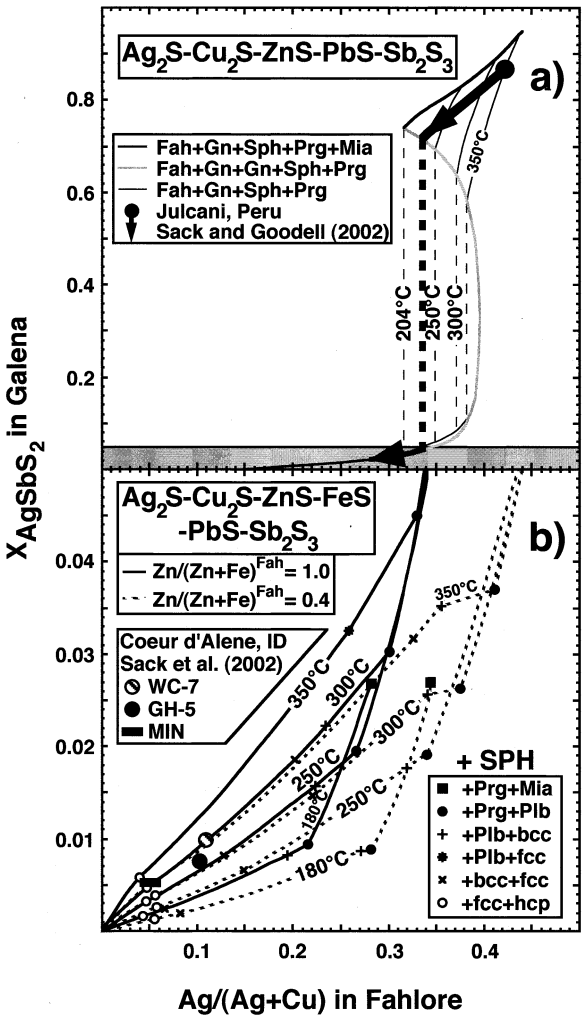

Fig. 6. Calculated mole fractions of $AgSbS_2$ in galena ($X^{Gn}_{AgSbS_2}$) and molar Ag/(Ag+Cu) of coexisting **Fah** in **Fah + Gn + Sph** assemblages in the simple systems **a**) Ag_2S-Cu_2S-ZnS-PbS-Sb_2S_3 and **b**) Ag_2S-Cu_2S-ZnS-FeS-PbS-Sb_2S_3. Calculations are based on the Ag_2S-Cu_2S-ZnS-FeS-Sb_2S_3 database, an asymmetric Margules model for $AgSbS_2$-Pb_2S_2 **Gn** solid solutions with $W^{Gn}_{AgSbS_2}$ = 27.1 and $W^{Gn}_{Pb_2S_2}$ = 10.5 kJ/gkw (Chutas, 2004), and the standard state properties of cubic $AgSbS_2$ given by Sack (2000). Explicit provision has not been made for saturation with diaphorite (~$Pb_2Ag_3Sb_3S_8$) or freieslebenite (~$PbAgSbS_3$). **a**) Compositions of fahlore and galena in the **Fah + Gn + Sph + Prg** assemblage (*thiner solid curves*) over the temperature range 150 to 350°C. Thicker solid curves and shaded line represent five-phase assemblages containing **Mia** and a second **Gn** phase (T_c = 454°C, $X^{Gn}_{AgSbS_2\ c}$ = 0.311), respectively. *Vertical dashed lines* connect binodal **Gn** pairs. *Arrowed path* emanating from black circle is a schematic path for the retrograde evolution of **Gn** and **Fah** from the "bonanza-Ag" zone from Julcani, Peru (Fig. 11; Sack and Goodell, 2002). **b**) Blow-up of shaded area in **a**) showing compositions for **Gn** and **Fah** in Ag_2S-Cu_2S-ZnS-PbS-Sb_2S_3 (solid curves) and Ag_2S-Cu_2S-ZnS-FeS-PbS-Sb_2S_3 (*dashed curves*) system assemblages with **Sph** and one of the minerals **Mia**, **Prg**, **Plb**, or **bcc**-, **fcc**-, or **hcp**-$(Ag,Cu)_2S$ solid solution. Points defined by four-phase curve intersections are labeled as indicated in legend; **Fah** in the Ag_2S-Cu_2S-ZnS-FeS-PbS-Sb_2S_3 system have molar Zn/(Zn+Fe) = 0.4, that of **Fah** from sample WC-7 from the West Chance vein of the Sunshine Mine (Sack et al., 2002). **Fah** from GH-5 from the Gold Hunter vein from the Lucky Friday Mine have molar Zn/(Zn+Fe) ~ 0.8. *Larger circles* are estimates for original **Gn** and **Fah** compositions for these samples. *Horizontal bar* represents the minimum weight percent Ag in Coeur d'Alene galena ores (cf., text) and the minimum molar Ag/(Ag+Cu) of Ag_2S-Cu_2S-ZnS-FeS-Sb_2S_3 **Fah** reported by Hackbarth (1984) and Trachte (1993).

form the halos beyond the envelope of main-stage metal mineralization and are a component of fluid emanations (Sack and Goodell, 2002). At Keno Hill, it is likely that high-Ag galenas in pyrargyrite ores provided the Ag, Sb, and S for the minerals stephanite, polybasite, acanthite, and wire silver (Boyle, 1965; Lynch, 1989a; Sack et al., 2003) during their epithermal alteration to anglesite ($PbSO_4$) and cerussite ($PbCO_3$).

On the practical side, the calibration given in Figure 6 might be used by mining geologists to evaluate Ag and Sb resources in Ag-Pb-Zn sulfide ore deposits. Even though galena has invariably "re-equilibrated" to low-Ag compositions in these ores, initial fineness of Ag in galena may be inferred, given primary hydrothermal mineralization temperatures and compositions of the more refractory fahlore. Combined with spatial information, such estimates of Ag fineness may then be used to evaluate the potential quantities of Ag and Sb derived from galena. In galena-rich deposits, this evaluation could be quite informative, particularly where Ag, and the more mobile Sb, have migrated large distances during retrogradation (i.e., lower-temperature stages of mineralization or mineral paragenesis during retrograde cooling). In deposits strongly zoned originally, spatial information and fahlore compositions might be combined directly to predict where zones of high-Ag galena were present. Database calibrations of mineral equilibria such as those illustrated here, or highlighted by Sack and Brackebusch (2004), are thus potentially useful tools for mine geologists, and they illustrate the use of fahlore as a indicator of petrogenesis, fineness, and mineralization potential for Ag and Au in polymetallic, hydrothermal ore deposits.

Despite the need to fine-tune the database for sulfide and sulfosalt solutions, expand the dimensionality of the chemical systems it encompasses (e.g., including Bi_2S_3, Ghosal and Sack, 1999), and add new mineral phases, it has been demonstrated that the thermodynamic models that comprise the database provide an excellent first-order accounting for the mineralogy of Ag-Pb-Zn sulfide ore deposits. Of course, further studies of phase equilibrium should be conducted to test the predicted partitioning of Fe and Zn between sphalerites and high-Ag fahlores and of Ag and Cu between fahlores and polybasite-pearceites. In the absence of direct observations, such constraints will provide important, albeit indirect, further constraints on the nature of fahlore miscibility gaps, and of the efficacy of the models comprising the database. It is hoped that the iterations between petrologic, theoretical, and laboratory and spectroscopic studies that will be required to refine this database will help to define new formats and paradigms for our analysis of hydrothermal precious metal sulfide deposits. Clearly we are well past the time when such databases should be incorporated into studies of hydrothermal ore-forming processes. Such integrations will presage the development of modern methods of mineral exploration and resource evaluation.

Acknowledgments—The support provided by NSF grant EAR-00-03679, discussions with Nathan Chutas and Lisa Hardy, and the comments and suggestions of three GCA reviewers and Dimitri Sverjensky are gratefully acknowledged.

Associate editor: D. Sverjensky

REFERENCES

Balabin A. I. and Sack R. O. (2000) Thermodynamics of (Zn,Fe)S sphalerite: a CVM approach with large basis clusters. *Mineral. Mag.* **64,** 923–943.

Boyle R. W. (1965) Keno Hill-Galena Hill lead-zinc-silver deposits, Yukon Territory. *Geol. Survey Can., Bull.* 111.

Bryndzia L. T. and Kleppa O. J. (1989) Standard molar enthalpies of formation of sulfosalts in the Ag-As-S system and thermochemistry of the sulfosalts of Ag with As, Sb and Bi. *Am. Mineral.* **74,** 243–249.

Chutas N. I. (2004) The Solubility of Silver Minerals in Galena. Ph.D. Thesis, University of Washington.

Chutas N. I. and Sack R. O. (2004) Ore genesis at La Colorada Ag-Zn-Pb deposit in Zacatacas, Mexico. *Mineral. Mag.* **68,** 923–937.

Ebel D. S. (1993) Thermochemistry of Fahlore (Tetrahedrite) and Biotite Mineral Solutions. Ph.D. Thesis, Purdue University.

Ebel D. S. and Sack R. O. (1989) Ag-Cu and As-Sb exchange energies in tetrahedrite-tennantite fahlores. *Geochim. Cosmochim. Acta* **53,** 2301–2309.

Ebel D. S. and Sack R. O. (1994) Experimental determination of the free energies of formation of freibergite fahlores. *Geochim. Cosmochim. Acta* **58,** 1237–1242.

Ghosal S. and Sack R. O. (1995) As-Sb energetics in argentian sulfosalts. *Geochim. Cosmochim. Acta* **59,** 3573–3579.

Ghosal S. and Sack R. O. (1999) Bi-Sb energetics in sulfosalts and sulfides. *Mineral. Mag* **63,** 723–733.

Goodell P. C. and Petersen U. (1974) Julcani mining district, Peru: a study of metal ratios. *Economic Geology* **69,** 347–361.

Grønvold F. and Westrum E. F. Jr. (1986) Silver(I) sulfide: Ag_2S. Heat capacities from 5 to 1000 K, thermodynamic properties and transitions. *J. Chem. Therm.* **18,** 381–401.

Grønvold F. and Westrum E. F., Jr. (1987) Thermodynamics of copper sulfides. I. Heat capacities and thermodynamic properties of copper (I) sulfide, Cu_2S, from 5 to 950 K. *J. Chem. Therm.* **19,** 1183–1198.

Grønvold F., Stølen S., Westrum E. F., Jr., and Galeas S. G. (1987) Thermodynamics of copper sulfides. III. Heat capacities and thermodynamic properties of $Cu_{1.75}S$, $Cu_{1.80}S$ and $Cu_{1.85}S$, from 5 to 700 K. *J. Chem. Therm.* **19,** 1305–1324.

Hackbarth C. J. (1984) Depositional Modeling of Tetrahedrite in the Coeur d'Alene District. Ph.D. Thesis, Harvard University.

Hardy L. S. (2002) Characterization of silver in Coeur d'Alene District ores: the missing component. In *Coeur d'Alene District Symposium* (ed. J. K. Duff and R. O. Laidlaw) Northwest Mining Association 108th Annual Meeting, Exposition and Short Courses 14-1.

Harlov D. E. and Sack R. O. (1994) Thermochemistry of polybasite-pearceite solutions. *Geochim. Cosmochim. Acta* **58,** 4363–4375.

Harlov D. E. and Sack R. O. (1995a) Ag-Cu exchange equilibria between pyargyrite, high-skinnerite and polybasite. *Geochim. Cosmochim. Acta* **59,** 867–874.

Harlov D. E. and Sack R. O. (1995b) Thermochemistry of Ag_2S-Cu_2S sulfide solutions: constraints derived from coexisting Sb_2S_3- and As_2S_3-bearing sulfosalts. *Geochim. Cosmochim. Acta* **59,** 4351–4365.

Keighin C. W. and Honea R. M. (1969) The system Ag-Sb-S from 600° to 200°C. *Mineral. Deposita* **4,** 153–171.

Knowles C. R. (1983) A microprobe study of silver ore in northern Idaho. In *Microbeam Analysis* (ed. R. Gooley), pp. 61–64, San Francisco Press.

Lynch J. V. G. (1989a) Large-scale hydrothermal zoning reflected in the tetrahedrite-freibergite solid solution, Keno Hill Ag-Pb-Zn district, Yukon. *Can. Mineral.* **27,** 383–400.

Lynch J. V. G. (1989b) Hydrothermal Zoning in the Keno Hill Ag-Pb-Zn Vein System: A Study in Structural Geology, Mineralogy, Fluid Inclusions and Stable Isotope Geochemistry. Ph.D. Thesis, University Alberta.

Lynch J. V. G., Longstaffe F. J., and Nesbitt B. E. (1990) Stable isotopic and fluid inclusion indications of hydrothermal paleoflow, boiling and fluid mixing in the Keno Hill Ag-Pb-Zn district, Yukon territory, Canada. *Geochim. Cosmochim. Acta* **54,** 1045–1059.

O'Leary M. J. and Sack R. O. (1987) Fe-Zn exchange reaction between tetrahedrite and sphalerite in natural environments. *Contrib. Mineral. Petrol.* **96,** 415–425.

Sack R. O. (1992) Thermochemistry of tetrahedrite-tennantite fahlores. In *The Stability of Minerals* (eds. N. L. Ross and G. D. Price), pp. 243–266, Chapman and Hall.

Sack R. O. (2000) Internally consistent database for sulfides and sulfosalts in the system Ag_2S-Cu_2S-ZnS-Sb_2S_3-As_2S_3. *Geochim. Cosmochim. Acta* **64,** 3803–3812.

Sack R. O. (2002) Note on "Large-scale hydrothermal zoning reflected in the tetrahedrite-freibergite solid solution, Keno Hill Ag-Pb-Zn district, Yukon" by J. V. Gregory Lynch. *Can. Mineral.* **40,** 1717–1719.

Sack R. O. and Brackebusch F. W. (2004) Fahlore as an indicator of mineralization temperature and gold fineness. *CIM Bull.* **97,** 78–83.

Sack R. O. and Ebel D. S. (1993) As-Sb exchange energies in tetrahedrite-tennantite fahlores and bournonite-seligmannite solid solutions. *Mineral Mag.* **57,** 635–642.

Sack R. O. and Goodell P. C. (2002) Retrograde reactions involving galena and Ag-sulphosalts in a zoned ore deposit, Julcani, Peru. *Mineral. Mag.* **66,** 1043–1062.

Sack R. O. and Loucks R. R. (1985) Thermodynamic properties of tetrahedrite-tennantites: constraints on the interdependence of the Ag↔Cu, Fe↔Zn, Cu↔Fe and As↔Sb exchange reactions. *Am. Mineral.* **70,** 1270–1289.

Sack R. O., Ebel D. S., and O'Leary M. J. (1987) Tennahedrite thermochemistry and metal zoning. In *Chemical Transport in Metasomatic Processes* (ed. H.C. Helgeson), pp. 701–731, D. Reidel.

Sack R. O., Kuehner S. M., and Hardy L. S. (2002) Retrograde Ag-enrichment in fahlores from the Coeur d'Alene mining district, Idaho, USA. *Mineral. Mag.* **66,** 215–229.

Sack R. O., Lynch J. G. V., and Foit F. F., Jr. (2003) Fahlore as a petrogenetic indicator: Keno Hill Ag-Pb-Zn district, Yukon, Canada. *Mineral. Mag.* **67,** 1023–1038.

Sack R. O., Fredericks R., Hardy L. S., and Ebel D. S. (2005) Origin of high-Ag fahlores from the Galena Mine, Wallace, Idaho, USA. *Am. Mineral.* (in press).

Schenck R. and von der Forst P. (1939) Gleichewichtsstudien an erzbinende sulfide. II. *Zeitschrift fur Anorg. Allgemeine Chem.* **241,** 145–157.

Schenck R., Hoffmann I., Knepper W., and Vogler H. (1939) Gleichewichtsstudien uber erzbinende sulfide. I. *Zeitschrift fur Anorg. Allgemeine Chem.* **240,** 178–197.

Skinner B. J. (1966) The system Cu-Ag-S. *Econ. Geol.* **61,** 1–26.

Trachte C. B. (1993) Geochemical Study of the Copper Vein, Sunshine Mine, Kellogg, Idaho. M.S. Thesis, Washington State University.

Verduch A. G. and Wagner C. (1957) Contributions to the thermodynamics of the systems PbS-Sb_2S_3, Cu_2S-Sb_2S_3, Ag_2S-Sb_2S_3 and Ag-Sb. *J. Phys. Chem.* **61,** 558–562.